# Ionization and self-association of unconjugated bilirubin, determined by rapid solvent partition from chloroform, with further studies of bilirubin solubility[1]

**Joon-Soo Hahm,[2,*] J. Donald Ostrow,[*] Pasupati Mukerjee,[†] and Lillian Celic[*]**

Gastroenterology Section, Department of Medicine,[*] V.A. Lakeside Medical Center and Northwestern University Medical School, Chicago, IL 60611, and School of Pharmacy,[†] University of Wisconsin, Madison, WI 53706

**Abstract** Our studies of equilibrium solubilization of crystals of unconjugated bilirubin (UCB) in buffered aqueous NaCl (1988. *J. Lipid Res.* **29:** 335–348) suggested that the two carboxylic pKa values were 6.8 and 9.3 and the solubility of UCB diacid was 0.1 $\mu$M. These data, however, were not ideal, due to possible effects of crystal size, metastability, 96-h incubation times with formation of polar derivatives, impurities in the bilirubin, and imprecision of analyses at low concentrations of UCB ([UCB]). In the present study, designed to determine the pKa values and self-association of UCB, these problems were minimized by solvent partition of UCB from solution in $CHCl_3$ into buffered aqueous NaCl. There was no crystal phase. Equilibrium was attained rapidly (10 min); UCB and $CHCl_3$ were highly purified; and accurate diazo assay of low [UCB] in the aqueous phase, [Bw], was achieved by concentrating the UCB through back-extraction into a small volume of $CHCl_3$. By determining effects on partition rations of varying the [UCB] in the $CHCl_3$ phase, [Bc], we could assess also the self-association of UCB species in the aqueous phase. Partition ratios (P = Bw/Bc) did not differ between initial and repeat extractions, indicating insignificant concentrations of polar UCB derivatives. Similar P ratios were obtained when equilibrium was approached from a supersaturated aqueous phase. At 21–25°C, $\mu$ = 0.15, the data (n = 76) fit the equation: $\log P = \log Po + \log[1 + 10^{(pH-A)} + 10^{(2pH-B)} + Bc \cdot 10^{(4pH-D)}]$; the bracketed terms reflect P for $H_2B^o$ (diacid), $HB^-$ (monoanion), $B^=$ (dianion), and $(B^=)_2$ dimer, respectively. Computer-fitted values for constants (±SD) were: Po = P for $H_2B^o$ = $5.79 \times 10^{-5}$; A = $pK_1$ = 8.12 ± 0.23; B = $pK_1 + pK_2$ = 16.56 ± 0.10; $pK_2$ = 8.44 ± 0.33; D = $pk_{22} + 2(pK_1 + pK_2) - \log(2Po)$ = 37.64 ± 0.07, and $k_{22}$ = 0.26 $\mu M^{-1}$ [formation constant of $(B^=)_2$ dimer]. In ancillary studies, multiple cycles of direct dissolution of UCB crystals revealed a progressive decrease in aqueous solubility of UCB as fine crystals were removed; this effect was minimal in $CHCl_3$. Unlike in water, moreover, varied UCB crystal forms had similar solubilities in $CHCl_3$, with [Bc] = 1.14 mM at saturation. As determined from $[Bc]_{sat} \cdot Po$, the aqueous solubility of $H_2B^o$ was 66 nM. In conclusion, *at physiological pH and ionic strength,* the two derived pKa values are approximately 8.1 and 8.4; $H_2B^o$ is the dominant UCB species, and $HB^-$, not $B^=$, is the dominant UCB anion; since the concentration of $B^=$ is so low, dimerization of $B^=$ is negligible; and aqueous solubility of UCB is less than 1% of its maximum concentrations in normal plasma (17 $\mu$M) and bile (35 $\mu$M). Since others have reported decreased uptake of UCB by erythrocytes, brain, mitochondria, and phospholipid vesicles as pH increases from 6.8 to 8.0, our data suggest that $H_2B^o$ is the species of UCB binding to these membranes. The ancillary studies emphasize the difficulties in interpretation of apparent ionization and solubility values derived from crystal dissolution studies.—**Hahm, J-S., J. D. Ostrow, P. Mukerjee, and L. Celic.** Ionization and self-association of unconjugated bilirubin, determined by rapid solvent partition from chloroform, with further studies of bilirubin solubility. *J. Lipid Res.* 1992. **33:** 1123–1137.

**Supplementary key words** unconjugated bilirubin • kernicterus (bilirubin encephalopathy) • gallstone pathogenesis

Unconjugated bilirubin (UCB), primarily as its calcium salts, is a major component of pigment gallstones (1–3). UCB toxicity to membranes and cells is responsible for the encephalopathy (kernicterus) that is associated with severe neonatal jaundice (4). It is, therefore, relevant to determine acid dissociation constants and self-association of UCB, as well as the limits of solubility of UCB in bile and plasma. We have recently published a study of the equilibrium and metastable solubility of UCB in simple

Abbreviations: UCB, unconjugated bilirubin; [UCB], concentration of UCB; W, water; C, chloroform. See Appendix for other abbreviations.

[1]This work was presented in part at the November, 1990 annual meeting of the American Association for the Study of Liver Diseases in Chicago, IL. (Abstract: *Hepatology.* 1990. **12:** 901.)

[2]Dr. Hahm was a Visiting Scholar from Hanyang University Medical School, Seoul, Korea, supported by a travel grant from that University. His current address is Division of Gastroenterology, Department of Medicine, Hanyang University, Seoul, Korea.

aqueous and bile salt solutions (5), determined by starting with crystals of UCB diacid ($H_2B^o$), or solutions of disodium bilirubinate ($Na_2B$), respectively. These studies revealed that massive metastable supersaturation occurred when $Na_2B$ was dissolved in bile salt solution and then rapidly buffered to pH below 9.0, and explained the wide differences in published values for bilirubin solubilities between studies performed in this manner (6–8) and those performed by dissolution of crystals of UCB diacid (9–14).

Computerized analysis of our data for equilibrium dissolution of UCB crystals over the pH range 4 to 11 (5) suggested that the two apparent pKa values of UCB were both high and widely separated, being approximately 7 and over 9, respectively. Thus, bilirubin monoanion ($HB^-$) appeared to be the predominant species of UCB anion at pH = 6.5–8.0, the physiological range for human bile (15). The accuracy of these apparent pKa values, however, is limited by possible inaccuracies in the measured solubilities, resulting from the inherent complexities of systems containing crystals. Thus, dissolution of crystals may be affected by the amounts (5, 11, 16), forms (5, 16–18), and sizes (19) of crystals, as well as by temporary development of metastable supersaturation during dissolution due to the presence of fine particles (5). In addition, despite the precautions of exclusion of light and oxygen (20), there was some degradation of UCB during the prolonged (96 h) incubations required to attain equilibrium (5), and the UCB crystals were not highly purified. The effects on the system of these degradation products and impurities are not known. Finally, in the studies performed without bile salts (Fig. 3 of ref. 5), the diazo-assay of the UCB dissolved at pH $\leq$7.0 yielded absorbances well below 0.010, and was too insensitive to measure dissolved UCB at pH <6.2, so that the solubility of $H_2B^o$ had to be estimated. As was noted in that paper (ref. 5, legend to Fig. 3), if this crude estimate was changed from 0.1 to 0.2 $\mu$M, the computer-fitted $pK_1$ increased from 6.83 to 7.25 and $pK_2$ decreased from 9.31 to 8.98. Thus, major uncertainties remained concerning the calculated pKa values for UCB.

For the above reasons, we have re-examined the acid dissociation and the self-association of UCB in aqueous solutions by rapid solvent partition from chloroform, determining the aqueous:chloroform partition ratio (P) over the pH range from 4 to 10. This system has the advantages of eliminating crystal effects by performing all operations with undersaturated UCB solutions (UCB fully dissolved in chloroform), minimizing UCB degradation because of the rapidity of the procedure (10 min), and permitting variations in the concentration of UCB in the chloroform phase ([Bc]), so that possible self-aggregation of UCB species at high concentrations (21, 22) could be assessed. By separately estimating saturation UCB solubility in $CHCl_3$, aqueous solubilities at any given pH value could be calculated from the partition ratio at that pH. The results differ from our prior studies with UCB crystals (5): $pK_1$ and $pK_2$ are within 0.6 units of each other, there is clear evidence of self-aggregation of the UCB dianion ($B^=$), and estimated UCB solubilities are lower than with crystals. Though the results still suggest that, at physiological pH values, the monoanion, $HB^-$, is the predominant UCB anion, the predominant UCB species is now the protonated diacid, $H_2B^o$.

## MATERIALS AND METHODS

### Materials

Crystalline UCB, lot #91687600, was purchased from British Drug Houses, Poole, Dorset, UK and purified by the method of McDonagh and Assisi (23). The purified UCB had a molar extinction coefficient in chloroform of 60.1 $mM^{-1}cm^{-1}$ and, by thin-layer chromatography, contained over 95% of the IX$\alpha$-isomer (23). Purified water, free of ions and organic contaminants, was prepared by serial passage of distilled water through charcoal, mixed-bed deionizing and Milli-Q systems (Continental-Millipore-Waters Co. Broadview, IL); its conductivity was less than $10^{-6}$ $\Omega^{-1}cm^{-1}$. Chloroform of reagent purity was purchased from J.T. Baker Co., Phillipsburg, NJ, and further purified by vacuum distillation at 53°C, the initial and final 10% volumes of distillate being discarded. The constant boiling distillate was washed successively with equal volumes of 0.1 N NaOH, 0.1 M $H_2SO_4$, and then five times with purified water. The washed chloroform was then stored under purified water in brown glass bottles in the dark for less than 72 h before use. Argon (Amerigas, Valley Forge, PA) was purified and presaturated with solvents by passage successively through a cartridge of activated charcoal, a Millex FG-50 filter (Millipore), and a container of purified chloroform and water. All other chemicals were reagent grade, obtained from Baker or Sigma. Buffers used (sodium salts) were citrate from pH 4 to 6, phosphate from pH 6 to 8, and borate above pH 8, all at ionic strength 0.10.

### Partition procedures (Fig. 1)

All solvents were deoxygenated by gassing with argon just before use. All procedures were performed under dim light. Partitions were performed at 21–25°C in 15- or 50-ml Pyrex glass tubes with tight-fitting Teflon-lined screw-caps (Cat. No. 45166, Kimble Co., Chicago Heights, IL). NaCl was added to the appropriate buffer to yield a total ionic strength of 0.15. This buffered stock solution was washed with an equal volume of pure chloroform, and then 3 to 40 ml was transferred to two tubes that had been prefilled with argon for 2 min. Purified UCB, approximately 1 mM, was dissolved in pure chloroform at 60°C, allowed to cool, and gassed with argon. The UCB–chloroform solution (3–12 ml) was then added to

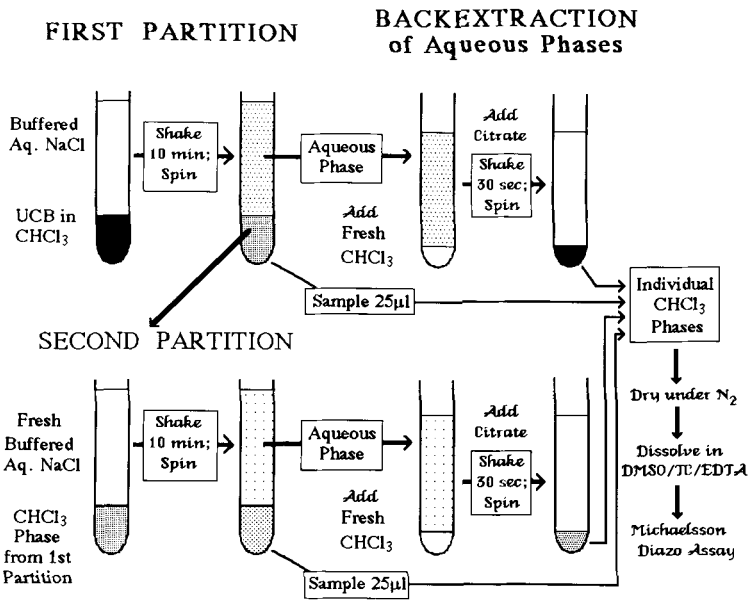


**Fig. 1.** Schematic illustration of the partition and back-extraction procedures.

the aqueous buffer–NaCl solution in the tubes, which were resealed immediately. The tubes were then inverted twice, the caps were briefly loosened to let off pressure of chloroform vapor, and the resealed tubes were gently shaken horizontally in a rotary shaker (Model 3520, Labline, Melrose Park, IL) at 60 cycles per min for 10 min. The tubes then stood vertically for 2 min to allow phases to settle, and were then centrifuged for 2 min at 1350 *g*. A measured quantity of the upper phase was carefully transferred to an argon-filled 15- or 50-ml partition tube, leaving 1 to 2 ml, so that the interphase and lower phase were undisturbed and hydration of the residual lower phase was maintained. Using a long, thin-tipped calibrated syringe (Scientific Glass Engineering, Austin, TX), 25-µl aliquots of lower phase were removed, uncontaminated by upper phase. The remaining upper phase and any interphase were then removed, and a second batch of the identical, chloroform-washed, buffered aqueous stock solution was then added to the residual lower phase from the first partition cycle. After again gassing with argon, the entire partition and sampling processes were repeated (cycle 2).

To determine whether the same P ratios were obtained by approaching equilibrium from the supersaturated state, reverse partitions (from aqueous into chloroform phases) were performed at pH 6.0, 7.0, 8.1, 9.1, and 9.3. In these studies, first cycle partitions were performed at higher pH values, and then the saturated aqueous phase was disequilibrated by gradually decreasing the pH by 0.3 to 2.4 units while extracting excess Bw into the chloroform phase. To do this, the equilibrated first partition system was constantly vortex-mixed while an equal volume of new buffer (pH 1 to 2 units lower than the first cycle) was added dropwise over a period of 5 min; the resultant slow decrease in pH minimized metastability (13). The tubes were then regassed with argon, sealed, and rotated horizontally for another 0.5, 2, or 4 h. This assured attainment of a new equilibrium at a P ratio at least 75% lower than the first cycle, despite the unfavorable gradient against which excess UCB moved from the low [Bw] to the higher [Bc].

### Assay of partitioned phases

Immediately after centrifugation, equilibrium pH of the upper phase was measured to the nearest 0.002 unit, using a digital pH-meter (Model 901, Orion, Cambridge, MA). Bilirubin assay was by the Michaelsson diazo reaction (24); data were used only from assays yielding a net $A_{600nm}$ of more than 0.05. Thus, the diazo assay could be performed directly on upper phases that contained more than 4 µM bilirubin (pH above 8.5), with an accuracy of ±3%. From measured volumes of upper phases with lower [Bw], as well as some samples from pH 8.5–9.1, pigment was back-extracted into 3.0 ml purified, washed chloroform, which was fully removed for analysis. Back-extraction of the aqueous phases with pH values between 7.5 and 9.0, was performed after adding 0.1 vol of 0.6 M sodium citrate buffer, pH 5.0, to bring the pH into a more favorable range for nearly complete transfer of the UCB into chloroform.

Measured volumes of the initial chloroform–UCB stock, the lower phases from the first and second partition cycles, and the lower phases from the back-extractions were each taken to dryness under a stream of nitrogen at

48°C. The residues were dissolved in 100–700 μl DMSO and 1 vol of stabilizer solution and 2 vol water were added. The stabilizer solution (10 mM $Na_2EDTA$/40 mM NaTC) protected the pigments against oxidation and precipitation, respectively. The Michaelsson assay was performed on this redissolved UCB, using two samples and one blank, 0.2 ml each, that contained 50 μl DMSO, 50 μl stabilizer, and 100 μl water.

To determine recoveries of UCB on back-extractions, a "dummy" back-extraction was performed on a control tube that contained the same buffer used in the partition, to which had been added a comparable concentration of UCB (freshly dissolved in 50–200 μl of 0.05 N NaOH). The quantity of UCB thus extracted was compared with the UCB content of an equal volume of the control solution, determined by direct diazo assay. UCB concentrations in the back-extracted upper phases from the partition assays were corrected for these recoveries, which averaged 92.6 ± 1.9% (mean ± SEM) for samples at pH 7.5–9.0 and 75.3 ± 3.7% for samples at lower pH values. Addition of citrate to the lower pH samples did not improve recoveries. At all pH values, however, the sum total of UCB recovered from the two equilibrated phases was always greater than 95% of the total amount of UCB introduced in the initial chloroform solution.

### Computer analyses

Best-fit linear regressions were determined for the plots of log P (where P = Bw/Bc) versus pH at pH values from 8.2 to 9.0, and of experimental versus calculated log P over the whole pH range (25). Using the VAX-11 computer (Digital Equipment Co.) at the University of Wisconsin, Madison, WI, with BMDP-AR, version 90, for derivative-free non-linear regression (BMDP Statistical Software, Inc., University of California, 1964 Westwood Blvd., Suite 202, Los Angeles, CA 90025), the data for P versus pH over the pH range from 4.1 to 9.8 were fitted to equation 1, whose full derivation is given in the Appendix (Model C):

$$\log P = \log Po + \log\{1 + 10^{(pH-A)} + 10^{(2pH-B)} + Bc \cdot 10^{(3pH-C)} + Bc \cdot 10^{(4pH-D)}\}. \quad Eq.\ 1)$$

The five terms within the large brackets represent, successively, the contributions of five UCB species in the aqueous phase: $H_2B^o$, $HB^-$, $B^=$, $(HB^-)(B^=)$ (mixed anion dimer), and $(B^=)_2$ (dianion dimer). The computer-derived constants are: Po, the partition ratio of $H_2B^o$; A = $pK_1$; B = $pK_1 + pK_2$; C = $pk_{12} + 2pK_1 + pK_2 - \log(2Po)$; and D = $pk_{22} + 2(pK_1 + pK_2) - \log(2Po)$. $K_1$ and $K_2$ are the ionization constants of the two -COOH groups of UCB, Bc is the concentration of UCB in the chloroform phase, and $k_{12}$ and $k_{22}$ are the association (formation) constants of the anion aggregates $(HB^-)(B^=)$ and $(B^=)_2$ respectively. As described later, the term containing C was found to be insignificant and was therefore dropped from the final equation used for derivation of the constants (equation 4, below).

As described in the Appendix, this mathematical model is based on the assumptions that only the monomer of $H_2B^o$ is present in the chloroform phase, and only this species partitions into the aqueous phase in accord with its intrinsic partition coefficient, Po. In the aqueous phase, $H_2B^o$ ionizes to form $HB^-$ and $B^=$, according to the two pKa values of UCB and the pH of the buffered aqueous phase (9), as represented by equation 2:

$$H_2B^o{}_c \leftrightarrow H_2B^o{}_w \leftrightarrow HB^-{}_w + H^+ \leftrightarrow B^={}_w + 2\ H^+. \quad Eq.\ 2)$$

Mathematical analysis of these equilibria (5, 9) yields the first three terms in equation 1. Since, however, most partitions were performed at [UCB] of 0.74–1.08 mM in $CHCl_3$ (65–95% of saturation (26)), association of the various bilirubin species becomes possible at the higher aqueous phase UCB concentrations, [Bw], obtained at higher pH values. As has been shown extensively for partitions of n-alkyl carboxylic acids (27–32) and planar organic dyes (33–37), formation of twin or mixed aggregates of the various UCB species in either phase will enhance the total solubility of UCB in that phase. The C and D terms in equation 1, therefore, are added to quantitatively express possible formation in the aqueous phase of the mixed anion aggregate, $(HB^- \cdot B^=)$ and the dianion dimer, $(B^=)_2$. The aggregated species, $(H_2B^o)_2$, $(H_2B^o)(HB^-)$, $(H_2B^o)(B^=)$ and $(HB^-)_2$, are not considered due to the very low concentrations of $H_2B^o$ and $HB^-$, rendering significant association unlikely (see Discussion and Appendix).

### Self-association of UCB dianions

To assess whether there was self-aggregation of $B^=$ or formation of the mixed aggregate $(HB^-)(B^=)$, P was determined at several high pH values with [Bc] varying from about 0.1 to 1.0 mM. To analyze such data, we note that, at pH values above 9.0, the $H_2B^o$ and $HB^-$ species together constitute less than 15% of the total Bw, and equation 1 simplifies to equation 3:

$$\log P = \log Po + \log\{10^{(2pH-B)} + Bc \cdot 10^{(3pH-C)} + Bc \cdot 10^{(4pH-D)}\}. \quad Eq.\ 3)$$

If there are no aggregates of $HB^-$ or $B^=$, the C and D terms may be deleted from equation 3, so that log P = log Po + 2pH − B, and (log P − 2 pH) = log Po − B should be approximately constant over a wide range of Bc values. If aggregates of $HB^-$ and/or $B^=$ are present, then P, as well as (log P − 2 pH) will increase with increasing Bc as well as pH. The (log P − 2pH) transformation is used to compensate for variations in final pH among partition tubes, since there are steep changes in P with minor changes in pH at pH values above 8.0.

### Multi-cycle crystal dissolutions in buffered aqueous solutions and in chloroform

Our prior study had shown that four different types of UCB crystals yielded vastly different aqueous solubilities, depending upon the degree of crystal orderliness as assessed by X-ray diffraction (Figs. 1 and 2 in ref. 5). To assess the role of crystal size on solubility, we performed two 96-h cycles of crystal solubilization in aqueous buffers, pH 8.0, 8.5, 9.0, and 9.3, using crystals prepared by evaporation of a $CHCl_3$ solution of UCB purified as described (23). After removal and diazo-analysis of the UCB dissolved in the supernatant from the first cycle, the residual crystals were incubated under argon with a fresh batch of the same aqueous buffer solution for another 96 h, and the analysis was repeated. The effect of temperature was studied by performing incubations both at 37°C and 25°C. In a second experiment, all first cycles were performed at pH 9.7–9.8, at which a greater proportion of the finer crystals were presumably removed, and the second cycles were then performed at the lower pH values used above.

To assess whether crystal forms and sizes would affect the solubility of UCB in chloroform, similar studies were performed with three cycles of dissolution in $CHCl_3$ of the four types of crystals, with markedly different degrees of orderliness, described in our 1988 paper (5). Crystalline UCB (Sigma), aged for 6 years, was utilized as the parent material for the other three preparations. Incubations were performed initially with 5 mg of crystals per ml chloroform, at 25°C under argon for 1 h per cycle. After each cycle, 0.4 ml of the solution was withdrawn, filtered through a $CHCl_3$-resistant, nylon Millipore, and the filtrate was analyzed by the modified Michaelsson method described above. After each of the first two cycles, the remaining 0.6 ml of $CHCl_3$ was aspirated, fresh $CHCl_3$ was added to a total volume of 1.0 ml, and the next cycle was performed under argon. After the 3rd cycle, however, the residual 0.6 ml $CHCl_3$ was incubated with the residual crystals for another 2 h and the solution then analyzed as above.

## RESULTS

### Preliminary studies

Partitions at 37°C revealed problems due to emulsion formation and the high volatility of $CHCl_3$; therefore, studies were performed at 21–25°C. Even at these temperatures, vigorous shaking favored emulsion formation that complicated sampling, whereas gentle rotational agitation, with the tubes horizontal to maximize interphase contact for partition, gave rapid equilibration without emulsion formation. With this approach, over the pH range from 4 to 10, maximal partition was attained by 8 min and remained stable up to 60 min when serially sampled without regassing with argon, but up to 4 h when argon was replaced after each sample was taken. Therefore, 10 min was selected as the standard partition time. It was also found important to avoid removing the entire upper phase after partition, since this led to disequilibration and clouding of the lower phases and emulsion formation. The lower phase could be sampled without contamination by upper phase if the narrow tip of the SGE syringe was inserted through the upper phase into the lower phase, air was expelled, the sample was aspirated, the syringe tip was withdrawn and wiped, and then air and a small portion of the fluid were expelled with the tip pointed upwards. Partition coefficients were unaffected by variations from 1 to 20 in the ratio of upper to lower phase volumes, so that upper phase volumes were selected to yield always sufficient UCB for accurate assay by back-extraction. At pH 7.5–8.2, upper phase UCB concentrations, [Bw], assayed by back-extraction, were always within 5% of [Bw] determined by direct diazotization. There were no significant differences in the P ratios obtained on the first and second cycles.

### Effects of [Bc] on P ratios at various pH values

**Fig. 2** shows that, at pH 9.5–9.9, where $HB^-$ constitutes less than 1% of UCB species, (log P – 2 pH) increased significantly as [Bc] increased from 0.1 to 1.0 mM, indicating self-aggregation of $B^=$ at pH values ≥9.5. By contrast, at pH 8.9 to 9.1, (log P – 2 pH) remained essentially constant as [Bc] varied over the same order of magnitude. This indicated that formation of $(HB^-)(B^=)$ or $(B^=)_2$ aggregates, if present, was too limited to influence the partition ratio in this pH range. Variations in [Bc]

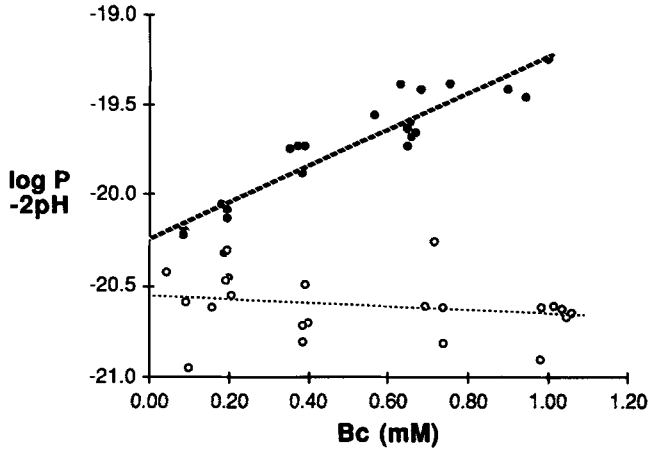


**Fig. 2.** Relationships between (log P – 2 · pH) and [Bc] (the equilibrium concentration of bilirubin in the chloroform phase) at pH 9.5 to 9.9 (upper curve, ●) and at pH 8.9 to 9.1 (lower curve, ○). The positive slope of the upper curve indicates self-association of $B^=$ at high pH. The lack of slope in the lower curve indicates no significant self-association of bilirubin species in either phase in this pH range.

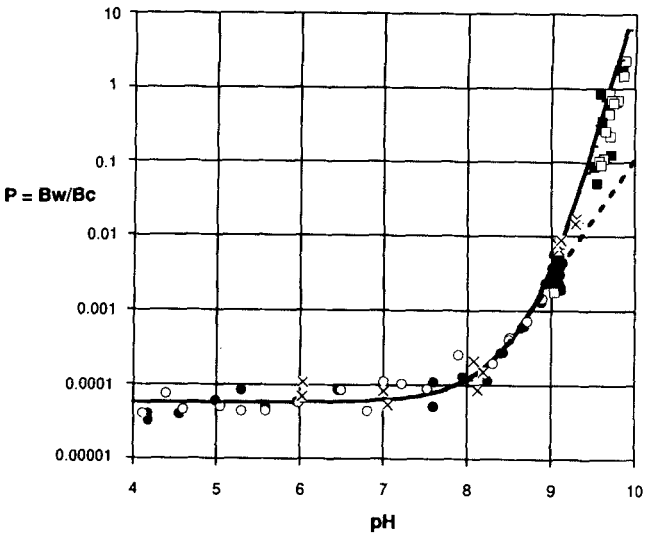


**Fig. 3.** Relationship between experimentally determined pH values and partition ratios (P = Bw/Bc) from chloroform into buffered aqueous NaCl solution, ionic strength = 0.15, at 23 ± 2°C. The black symbols represent data for the first partition cycle, the open symbols data for the second partition cycle in which the residual chloroform (C) phase from cycle 1 was repartitioned with fresh aqueous (W) phase. × represents partition ratios obtained by separate reverse partitions from W into C phases, achieved by a second cycle of equilibration after gradually decreasing the pH of the W phase obtained after the first cycle. There is no significant difference between the two cycles of partition from C to W phases, or from the reverse partitions from W to C phases. Circles, [Bw] assayed by back-extraction; squares, [Bw] assayed by direct diazotization. The solid curve represents the calculated values from pH 4.1 to 9.5, derived from equation 4, using the computer-fitted parameters. The dashed line represents the steep portion of a curve above pH 8.2, with the D term for dianion dimers of UCB omitted from equation 4. Upward deviation of the experimental data above pH 8.2 is due to dimerization of bilirubin dianions.

likewise did not affect P at lower pH values (data not shown), indicating no significant formation of the aggregates $(H_2B^o)_2$, $(H_2B^o)(HB^-)$, $(H_2B^o)(B^=)$, or $(HB^-)_2$.

### Partition from chloroform into aqueous phase at pH 4.2 to 9.8 and computer analysis of the data

The relationships of P to pH values are shown on a semi-logarithmic plot in **Fig. 3**. Log P increased slightly as pH increased from 4.0 to 7.5, but more steeply at higher pH values. In the pH range of 8.2 to 9.0, log P increased linearly with increasing pH, with a slope that approximated 2.0, as expected when both carboxyl groups of UCB are dissociating concurrently (12). From pH 9.0 to 9.8, the slope increased to values above 2.0, compatible with dimerization of $B^=$ in the aqueous phase (29, 30, 32–37). Above pH 9.8 (not shown), the slope increased even more steeply, consistent with aggregation of $B^=$ into even larger multimers (34–37).

In computer-fitting the data from pH 4.2 to 9.8, it was found that the C term from equation 1 was insignificant and its exclusion had no detectable effect on P ratios. The final computer-fitting, yielding the curve in Fig. 3, was performed, therefore, with equation 4, an abbreviated form of equation 1 that omits the C term for $(HB^-)(B^=)$:

$$\log P = \log Po + \log \{1 + 10^{(pH-A)} + 10^{(2pH-B)} + Bc \cdot 10^{(4pH-D)}\} \quad Eq.\ 4)$$

The computer-derived values were (mean ± SD): log Po = −4.237 ± 0.046, Po = $5.79 \times 10^{-5}$, A = $pK'_1$ = 8.12 ± 0.23, B = $pK'_1 + pK'_2$ = 16.56 ± 0.10, $pK'_2$ = 8.44 ± 0.33, and D = $pk_{22} + 2(pK_1 + pK_2)$ − log(2Po) = 37.64 ± 0.07. The aggregation constant for $(B^=)_2$, $k_{22}$ = 0.26 $\mu M^{-1}$.

Fig. 3 and **Fig. 4A** demonstrate that equation 4 yielded an excellent fit of the data, with a [residual root mean square]$^{0.5}$ of 0.191. By contrast, omission from equation 4 of the D term, which was the only term containing Bc as a variable, led to a much greater [residual root mean square]$^{0.5}$ of 0.411, failure of convergence for the A constant, and (Fig. 4B) very poor fitting at pH values above pH 9.0. This confirms the importance of including the D term for dimerization of $B^=$ in the aqueous phase.

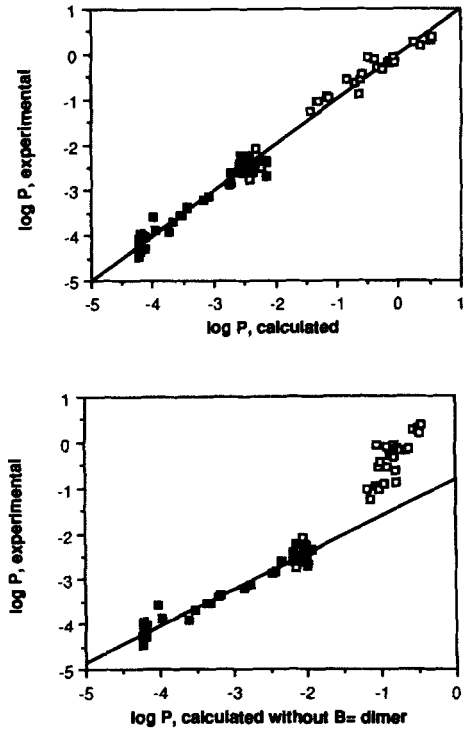


**Fig. 4.** Relationships between experimentally determined partition ratios (ordinate), and partition ratios calculated from equation 4 (abscissa), using the computer-fitted constants. In the upper graph (A), the full equation 4 is used, with an excellent fit throughout the entire range of data ($r$ = 0.99, [residual root mean square]$^{0.5}$ = 0.191). In the lower graph (B), the D term in equation 4 (representing the $B^=$ dimer) is omitted from the analysis, resulting in a marked upward deviation of experimental above calculated values, and a much larger [residual root mean square]$^{0.5}$ = 0.411. This indicates the importance of incorporating the $B^=$ dimer into the analysis. In both graphs, ■ = partition ratios determined by back-extraction and □ = those determined by direct diazo assay. Note the excellent agreement between the two assays in the range from log P = −2 to −3, where both assays could be applied.

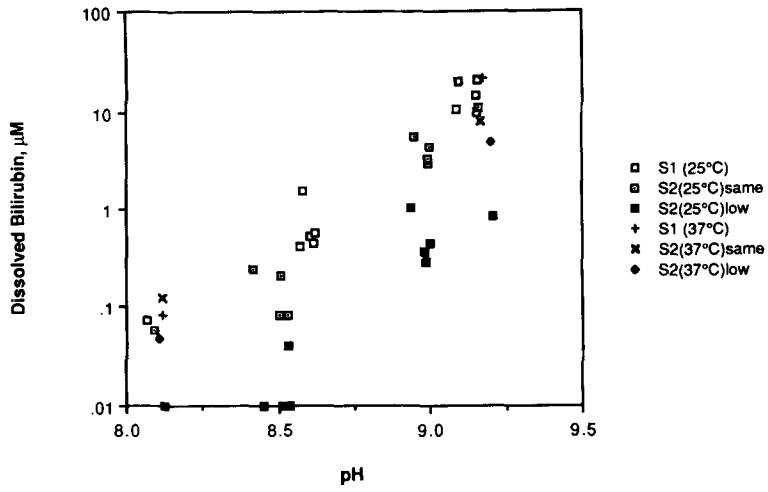


**Fig. 5.** Solubilization (96 h at pH = 8 to 10) of UCB crystals, prepared by evaporation of a chloroform solution of UCB. Squares represent studies at 25°C; +, × and ♦ studies at 37°C. S1, UCB crystals solubilized after first cycle (□, +). S2, solubilization during second 96-h cycle of residual crystals from first cycle. S2 same, second cycle performed at pH similar to first cycle (□, ×). S2 low, second cycle performed with aqueous buffer at pH values well below first cycles done at pH 9.7 to 9.8 (■, ♦).

### Reverse partition from aqueous into chloroform phase

Fig. 3 also shows partition ratios, obtained by first performing a partition from the C into the W phase at pH 9.6, 9.3, 9.1, 8.7, or 8.4, and then repartitioning the equilibrated system as the pH of the W phase was gradually dropped to pH 9.3, 9.0, 8.1, 7.0, and 6.0, respectively. As a result, attainment of the second equilibrium required reverse transfer of UCB from the W to C phase. P from these reverse partitions straddled the fitted curve at all five final pH values (Fig. 3), with no differences among partitions equilibrated for 0.5, 2.0, or 4.0 h. This indicated that the same equilibria were reached whether the excess UCB was initially present in the C or W phase, and whether the aqueous phase was initially under- or supersaturated.

### Two-cycle dissolution of UCB crystals in aqueous buffer

**Fig. 5** shows that second cycle aqueous solubilities were greatly affected by prior removal of fine particles with a first cycle of dissolution. At 25°C, second cycle solubilities were modestly lower if the first cycle had been done at a similar pH value, but an order of magnitude lower if a greater proportion (>15%) of the original crystals had been dissolved during a first cycle performed at a higher pH (9.6–9.8). At 37°C, the decreases in dissolution, during second as compared with first cycles, were less striking. First cycle solubilities were similar at both temperatures.

### Three-cycle dissolution of four types of UCB crystals in chloroform

As shown in **Fig. 6**, four types of UCB crystals (5) showed less than twofold differences in chloroform solubility at 25°C. The greatest solubility was shown by crystals flocculated by acidifying a metastable solution formed by adding DMSO-solubilized UCB to water. UCB crystals formed by evaporation of a solution of UCB in chloroform yielded the lowest solubility. The parent, aged crystals, and those flocculated by addition of $CHCl_3$-solubilized UCB to petroleum hydrocarbon (PHC) yielded intermediate solubilities. For the PHC and DMSO crystals, the second and third 1-h cycles yielded progressively lower

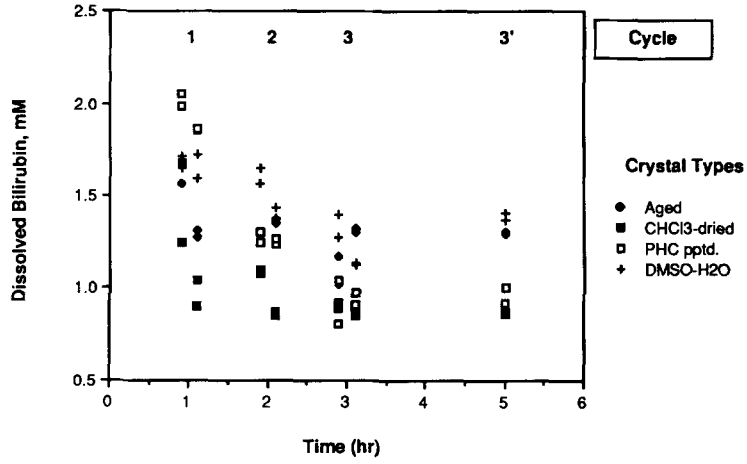


**Fig. 6.** Multicycle solubilization of different forms of UCB crystals in chloroform at 25°C. Three cycles were performed of 1 h duration each, the second and third cycles utilizing the residual crystals from the preceding cycle. After 1 h of the third cycle, half the chloroform solution was incubated with the residual crystals for another 2 h. Symbols represent different forms of UCB crystals, prepared as described in (5); ♦ = original aged UCB crystals from Sigma Co., used to prepare the other three forms of crystals; ■ = crystals formed by evaporation of a chloroform solution of UCB; □ = crystals formed by addition of petroleum ether to a chloroform solution of UCB; + = crystals formed by acidification of a suspension formed by adding to water a solution of UCB in DMSO.

solubilization than each preceding cycle, which preferentially dissolved smaller and less-ordered crystals (5, 16–19). By contrast, the aged and $CHCl_3$-dried crystals exhibited constant solubilities throughout successive cycles. For the third cycle, incubation of each crystal form for an additional 2 h yielded solubilities comparable to that obtained after 1 h, suggesting that equilibrium had been attained. The mean solubility in $CHCl_3$ of the aged and $CHCl_3$-dried forms of UCB, averaged from the third cycles, was 1.06 ± 0.20 mM (mean ± SD), similar to the value of 1.14 ± 0.04 mM we obtained previously by 72-h isoextraction (33) of UCB from $CHCl_3$ into multiple buffered aqueous solutions in the presence of excess $CHCl_3$-dried UCB crystals (26). The mean solubility of the comparable $CHCl_3$-dried crystals (0.88 ± 0.02 mM) was, however, 23% lower.

## DISCUSSION

### Methodological considerations

The application of solvent partition to assess the ionization constants, aqueous self-association, and apparent solubility of an amphiphile requires scrupulous attention to methodological detail. In the present studies, the UCB and chloroform were highly purified, and the chloroform phase was pre-washed with water to remove any polar derivatives (28, 29) formed from bilirubin or chloroform. To minimize bilirubin oxidation and dipyrrole exchange, both of which may result in the formation of more polar, diazo-reactive derivatives (20), the partitions were completed in 10 min in dim light, under argon, using solvents previously purged of oxygen with argon. The success of these maneuvers was attested by stable partition ratios from the C phase to the W phase over a period of 4 h, close agreement of partition ratios derived from the first and second cycles of aqueous extraction from the same chloroform phase, and total recoveries of UCB (sum of both phases) in excess of 95% at all pH values and UCB concentrations. Of great importance, the attainment of closely similar partition ratios on reverse partitions of UCB from the W to the C phase renders it likely that equilibrium was achieved during the 10-min partitions from chloroform into aqueous buffers, despite the high density of $CHCl_3$. Note that Brodersen and Vind (38), using reverse partition into $CHCl_3$, obtained a similar P of 1.0 at pH 9.7, that likewise decreased steeply with decreasing pH.

Measurement of the very low concentrations of UCB in the aqueous phase at pH values below 7.5 was achieved by concentrating the pigment up to 100-fold by back-extraction from 20 to 60 ml of aqueous phase into 3.0 ml of chloroform, followed by evaporation of the chloroform and redissolution of the dried pigment in 0.4–0.7 ml of DMSO/water containing bile salt and EDTA as stabilizers. Thus, all diazo assays were performed on final solutions that contained at least 4 μM UCB, yielding $A_{600}$ values of at least 0.050 and an accuracy of diazo assay of ±3% (20). At pH 7.5–8.2, upper phase UCB concentrations were assayed by both direct diazotization and by back-extraction; the agreement of the two assays within 5%, as well as the excellent recoveries (mean 93%) on dummy back-extractions in this pH range, validates the back-extraction method. The lower recoveries (mean 75%) obtained on dummy back-extractions at pH values below 7.5 are thus likely due to the much larger volume of the aqueous as compared to $CHCl_3$ phases. Although the aqueous phase UCB concentrations, [Bw], determined by back-extraction, were corrected by the recoveries from comparable standard UCB solutions on parallel "dummy" back-extractions, the less than full efficiency of back-extraction means that the [Bw] at pH <7.5 probably have lower accuracy than those at higher pH values. Nonetheless, they are vastly more accurate than the aqueous solubilities of UCB crystals determined in our prior paper (5), in which the diazo $A_{600}$ values for studies at pH <7.0 were 0.001 to 0.010. By contrast, at pH values above 8.0, the measurement of [Bw] by direct diazo assay is accurate within ±3%, but errors in measurement of pH become paramount, due to the steep increments in P with small increases in pH values. The random nature of these errors had little influence on the overall data analysis, as attested by the excellent fit of experimental and computer-calculated partition ratios over the entire pH range (Fig. 4A).

### Solvent interactions

To apply the results from our partition data to assess the behavior of UCB in aqueous solutions in the absence of $CHCl_3$, it is necessary to examine the possible effects of the mutual solubility of the solvents (27–29) on the thermodynamic activity of $H_2B^o$, its dissociation constants in the aqueous phase, and the self-association of the anions therein. As shown below, the effects are expected to be small. At 23°C, the solubility of water in chloroform is <0.1% (v/v) and of chloroform in water is 0.55% (v/v) (39). The effect of the minor component on the activity of $H_2B^o$ can be estimated using the theory of the solubility of uncharged molecules in mixed solvents (40). The solubility, S, in $CHCl_3$-saturated water should then be related to the true solubilities in pure water ($S_w$) and pure $CHCl_3$ ($S_c$) by the equation: $\log S = \log S_w + (\log S_c - \log S_w) \cdot f$, where f is the volume fraction of $CHCl_3$ in water. From estimated values of $1.14 \times 10^{-3}$ M for $S_c$, $6.6 \times 10^{-8}$ M for $S_w$ and 0.0055 for f, the $S/S_w$ ratio is calculated to be 1.06. This 6% effect is not negligible, but is small compared with the 11% standard error of Po. The effect of dissolved water on the activity of $H_2B^o$ in the $CHCl_3$ layer is calculated to be much less because f, in this case, is less than 0.001. The relatively small effect of low amounts of added solvents on the solubilities of non-

electrolytes has been demonstrated previously (39). As an example, the solubility of naphthalene, 0.030 g/kg in water, increases to only 0.044 g/kg in 5% ammonia, even though the solubility is 4,000 times higher in 100% ammonia (39). The effects of dissolved $CHCl_3$ on the dissociation constants of $H_2B^\circ$ and the self-association of UCB anions in the aqueous phase are expected to be small, in view of the negligible effects reported, respectively, on the dissociation constants of two organic acids, benzoic acid and *p*-nitrophenol (41), and on the hydrophobic self-association of methylene blue (33).

To be considered also is the possible formation of solvates of UCB with $CHCl_3$ or water, which might have different partition properties than the unsolvated species. Since the activity of each solvent in the other phase is constant in all studies, the concentration of any UCB solvate, if it exists, should be a constant fraction of the total [UCB] in the relevant phase. Therefore, the constancy of P over wide ranges of [Bc] indicate that such solvates, if present, are low in concentration, and/or have little effect on the relation of P to [Bc]. As discussed later (Fig. 8), data on association of UCB with phosphatidylcholine vesicles at varied pH values (42), obtained in the absence of $CHCl_3$, are consistent with our partition-derived pKa values. This suggests that a $CHCl_3$ solvate of UCB, if it exists, has minimal effects on the relationships of P to pH.

### Association of UCB species

Self-association of $B^=$ in the aqueous phase at high pH values was evidenced by the increasing slope of the plot of P versus pH as pH increased (Fig. 3), the increasing values of (log P − 2 pH) as [Bc] increased (Fig. 2), and the marked deviations of theoretical from experimental P ratios if the dimerization term was omitted from equation 4 (Fig. 4B). At pH 9 or below, however, there were no deviations above or below the theoretical plot for log P versus pH and P did not vary with [Bc]. This confirmed that there was no significant dimerization of $H_2B^\circ$ in either phase, as reported in studies using other methods (43), and that formation of $(HB^-)_2$, $(H_2B^\circ)(HB^-)$ and $(H_2B^\circ)(B^=)$ if present, had no significant influence on the partition ratios obtained. Removal of the C term in equation 1 had no effect on the computer fit of our data, indicating that $(HB^-)(B^=)$, if present, was not a significant species in our system.

Our data thus indicate that the only UCB complex that has any significant effect on the total aqueous solubility of UCB up to pH 9.8 is the dimer, $(B^=)_2$, but it is a negligible species at physiological pH values (pH <8.3, **Fig. 7**). Formation of $(B^=)_2$ had been deduced previously by others (21, 22), based on spectral changes with varying [UCB]. Our derived dissociation constant for the $(B^=)_2$ dimer, 3.85 $\mu$M, is close to the value of 1.5 $\mu$M, derived at pH 10.0 by Carey and Koretsky (22), but is very different from the value of 83 $\mu$M derived at pH 8.3 by Brodersen

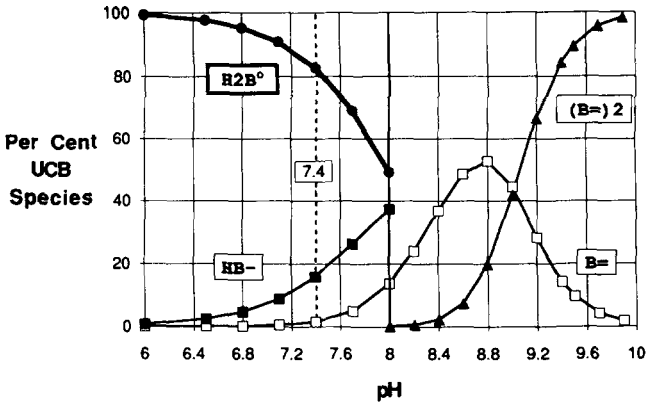


**Fig. 7.** Per cent bilirubin species at pH values from pH 6.0 to 9.9, calculated from the computer-fitted calculated pKa values of bilirubin, 8.12 and 8.44. $H_2B^\circ$, ●, protonated bilirubin diacid; $HB^-$, ■, bilirubin monoanion; $B^=$, □, bilirubin dianion monomer; ▲, bilirubin dianion dimer $(B^=)_2$. Throughout the physiological pH range for bile (6.0 to 8.0), $H_2B^\circ$ was the dominant species and $HB^-$ the dominant bilirubinate anion. Dianion dimer was detectable only at higher pH values (above 8.2). For purposes of clarity, the $H_2B^\circ$ and $HB^-$ species are omitted above pH 8.0.

(21). The latter value, however, was based on a model that assumed that $B^=$ was the only anion species present, whereas our results indicate that, at pH = 8.3, $B^=$ constitutes only 30% of total [UCB] and $HB^-$ is the predominant species.

### Apparent pKa values and species of UCB in aqueous solutions

In sharp contrast to our study of solubilization of UCB crystals (5), the present analysis suggests that the two pKa values of UCB are close together and both above pH 7.9. Carboxyl groups, however, usually have pKa values below 5.0. Our unexpectedly high pKa values are probably the result of retarded dissociation of the protons due to the trio of internal hydrogen bonds between each carboxyl group and the -CO-NH- and >NH groups of the opposite dipyrrylmethene rings (5, 43–45). When this internal bonding is broken, e.g., by dissolution of UCB in dimethyl sulfoxide or dimethylformamide, titrimetric and $^{13}$C-NMR studies yield, as expected, pKa values between 4.5 and 5.0 (46). In the present partition studies, the derived pKa values (±SD) were $pK_1 = 8.12 \pm 0.23$ and $pK_2 = 8.44 \pm 0.33$. The analysis yields a less accurate estimate of the individual pKa values than of their sum, $pK_1 + pK_2 = 16.56 \pm 0.10$, which is similar to the sum of 16.15 obtained in our prior studies of crystal dissolution (5). In the present study, however, $pK_1$ is quite close $pK_2$, contrasting with the difference of 2.5 pH units obtained previously (5).

To examine the relation between $pK_1$ and $pK_2$, we note that, for symmetrical dibasic acids such as oxalic acid and its homologues, $pK_2 - pK_1 = \log 4 + E$ (47). The factor 4 is a statistical factor, arising from the assumption that

the two possible isomers of $HB^-$ are equally likely to form when $H_2B^o$ ionizes and are equally likely to ionize in turn to yield $B^=$. E represents the effect of the electrical field of one ionized group on the other (47). The magnitude of E decreases rapidly as the distance increases between the dissociable groups. For example, Δ pK for $HOOC-(CH_2)_n-COOH$ is 2.85 when n = 1, 1.43 when n = 2, and only 0.85 when n = 4 (47). Molecular models of $H_2B^o$ (43) indicate that its dissociable-COOH groups are sufficiently far apart for E to be near zero, so that $(pK_2 - pK_1)$ should be close to the minimum value of log 4 or 0.60. Assuming that E = 0, our derived sum of 16.56 for $(pK_1 + pK_2)$ leads to estimates of 7.98 for $pK_1$ and 8.58 for $pK_2$, which are within 1 SD of our experimentally derived pKa values. The experimental data are thus consistent with the concept that the two dissociable groups in $H_2B^o$ have equivalent structures. The pKa values of 6.8 and 9.3, obtained previously with our crystal dissolution studies (5), gave a Δ pK of 2.5, which is incompatibly large for this concept. Those unsatisfactory pKa values resulted from the analytical problems discussed above, and from the misleading solubilities obtained with crystal dissolution studies, discussed below.

Using the experimental pKa values of 8.12 and 8.44 and the dimerization constant of 0.26 $\mu M^{-1}$, one may calculate from equation 4 the proportions of the individual UCB species (Fig. 7). As shown in Fig. 7, at biliary pH values of 6.0–8.0, $H_2B^o$ is the dominant species and $HB^-$ the dominant anion. There is no significant $B^=$ at pH values below 7.0 (i.e., in gallbladder bile) and less than 14% at pH values up to 8.0 (i.e., in hepatic bile). As noted earlier, the $[B^=]_2$ dimer is virtually absent in this physiological pH range, where the dominant feature is a decrease in the proportion of $H_2B^o$ and increase in the proportion of $HB^-$ with increasing pH. Independent confirmation of this concept and of our pKa values is the data in **Fig. 8**, showing that application of our pKa values predicts quite well the data points obtained by Tipping, Ketterer, and Christodoulides (Fig. 10 in ref. 42) if it is assumed that $H_2B^o$ is the species that was binding. They showed markedly decreased binding of 10 μM bilirubin to 100 μM egg lecithin vesicles (a model membrane) as pH increased.

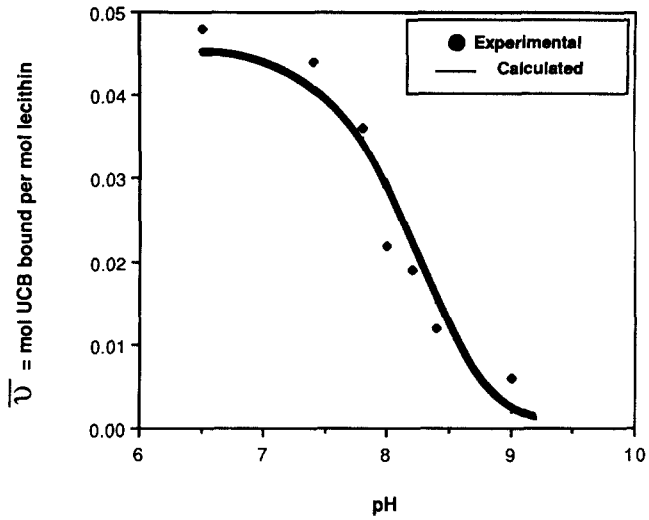


**Fig. 8.** Binding of UCB to lecithin vesicles, comparing mol UCB bound per total mol lecithin ($\bar{\nu}$), calculated using our computer-derived pKa values for UCB of 8.12 and 8.44 (▬), with experimentally derived data (●) from Tipping et al. (ref. 42, Fig. 10). In this analysis, at each pH value, the concentration of unbound $H_2B^o$ in the presence of vesicles is assumed to be equal to the $[H_2B^o]$ in the aqueous phase of our partition studies. Our derived value for $\bar{\nu}$ is then calculated from the relationship, $\bar{\nu} = [H_2B^o] \times 8.5 \times 10^{-3}\ M^{-1}$, which assumes a constant ratio for $\bar{\nu}/[H_2B^o]$. The excellent agreement between our calculated curve and Tipping's experimental values supports the validity of our partition data and the pKa values derived therefrom.

### Crystal dissolution studies

Our new studies with UCB crystals were performed to clarify several issues, the most important being the discrepancy in the pKa values derived from our prior crystal dissolution studies (5) as compared with the present data. The second issue relates to the variability of solubilities determined from crystal dissolution, as shown also in our prior paper (Fig. 2. in ref. 5). We noted there the marked variability in aqueous solubility resulting from differences in crystal orderliness. Particle size effects can be very serious also, since the data in Fig. 5 of the present paper showed that removal of finer, more soluble crystals by one cycle of dissolution reduced the aqueous solubility of the residual crystals in the second cycle.

The solubilities of fine particles are expected to be higher than those of large particles (48, 49) by a factor $X = \exp(2\gamma V/RTr)$, in which γ is the interfacial tension of the solid against water, V is the molar volume of the solute, R is the molar gas constant, T is the absolute temperature, and r is the radius of the particles (assumed to be spherical). Using rough estimates of 40 ergs/cm² for γ and a volume of 550 ml/mol for $H_2B^o$, the values of X at 25°C are calculated to be 1.19, 1.80, and 5.84 for particle diameters of 0.20 μm, 0.06 μm, and 0.02 μm, respectively. These calculations indicate that X can indeed be quite high in water, and our data in Fig. 5 confirm this, showing that solubility of UCB crystals in aqueous buffer can be decreased by as much as an order of magnitude when fine particles are removed by prior dissolution.

Effects of particle size and crystal orderliness are confirmed also by the studies of crystal dissolution in $CHCl_3$ (Fig. 6), in which crystals flocculated by the DMSO and PHC methods showed decreasing solubility on successive cycles. However, removal of fine particles from the $CHCl_3$-dried UCB crystals, which profoundly decreased their aqueous solubility (Fig. 5), had negligible effects on their solubility in $CHCl_3$ (Fig. 6). This is consistent with the much lower interfacial tension expected between UCB crystals and chloroform. There was, however, some vari-

ability of $CHCl_3$ solubility among different crystal forms, so that crystal order effects were not negligible, and may account for the much higher solubility of UCB in $CHCl_3$ (2.5 mM) reported by Brodersen (12), as compared with ours (1.14 mM) (26). These effects in $CHCl_3$, however, were small compared to our report of variation of up to 20-fold in direct aqueous solubilities of different crystal forms of UCB (Fig. 2 in ref. 5).

### Aqueous UCB solubilities calculated from partition data

In prior studies involving 72 h of isoextraction of UCB from $CHCl_3$ into a range of aqueous buffers (26), we had obtained a mean value of 1.14 ± 0.04 mM as the saturation solubility of UCB in $CHCl_3$ in the presence of excess UCB crystals. This value is near the mean of the third cycle values for direct $CHCl_3$ solubilities shown in Fig. 6, performed in the absence of an aqueous phase. This indicates that the presence of an aqueous phase has little influence on the solubility of UCB in $CHCl_3$, and mitigates also against a significant influence on P Ratios of any possible hydrate of UCB.

The above considerations permit us to use the above solubility of UCB in $CHCl_3$ (1.14 mM) as [Bc] at saturation, multiplied by P at each pH, to calculate the solubilities of UCB in water (**Fig. 9**). These partition-derived aqueous solubilities are much more reliable and uniformly much lower than those that we (5) and Moroi, Matuura, and Hisadome (14) obtained from crystal dissolution. These lower UCB solubilities obtained by partition (Fig. 9) are not due to the lower temperatures used (21–25°C), as compared with our prior crystal dissolution studies (37°C) (5) as there were no significant differences in UCB crystal solubility between these temperatures (Fig. 5). Lower solubilities in the present study might be related in part to absence of surface-active impurities from the more highly purified UCB that was utilized. As discussed above, the most important factors are probably the effects of crystal size and orderliness.

The aqueous UCB solubilities reported by Brodersen (11, 12) are at least an order of magnitude lower than ours at pH values below 8.0, but he likely failed to reach equilibrium since he used relatively small excesses of crystals incubated for only a few hours. Our data suggest that the maximum aqueous solubility of $H_2B^o$ is 66 nM at 25°C. As shown in Fig. 9, total UCB solubility increased moderately with increasing pH to only 0.08 μM at pH 6.8, the maximum pH of normal human gallbladder bile (15, 50), and to 0.17 μM at pH 8.0, the maximum pH of human hepatic bile (51).

### Pathophysiological significance: kernicterus and pigment gallstone formation

*Kernicterus.* Brodersen (52) and Brodersen and Stern (4) have proposed that if plasma becomes markedly supersaturated with unbound $H_2B^o$, as occurs if the total [UCB] is sufficiently high and the pH is sufficiently low, then $H_2B^o$ aggregates and precipitates in the phospholipid membranes of brain neurones (53), causing bilirubin encephalopathy (kernicterus) (4, 52, 54). This hypothesis, however, is based on the solubility data of Brodersen (11) from which are derived their concepts that the aqueous solubility of UCB at pH 7.4 is $<0.01$ μM and that $B^=$ is the only bilirubin anion present in physiological systems (4, 11, 52). Our present data suggest, rather, that maximum aqueous UCB solubility at pH 7.4 is actually close to 0.1 μM (Fig. 9) and that there is little unbound dianion present at this pH, either monomeric or dimeric (Fig. 7). If the dissociation constant for binding to the first site on plasma albumin is $1.5 \times 10^{-8}$ M (12), our data suggest

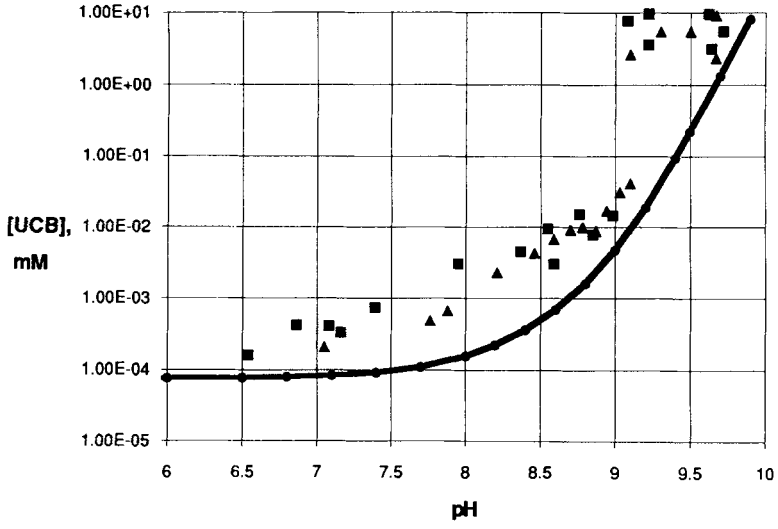


**Fig. 9.** Relationships between equilibrium saturation solubilities of unconjugated bilirubin, [UCB], and pH, comparing current solvent partition data (lower curve, —●—) with data from our prior study (5): ■ = dissolution of solid bilirubin crystals; ▲ = residual solubility after rapid acidification of dissolved disodium bilirubinate. The lower curve was derived from equation 4, using the computer-fitted constants: $pK_1$ = 8.12, $pK_2$ = 8.44, log Po = −4.2368, $pk_{22}$ = 3.589, and multiplying the resultant $P_{calculated}$ by 1.14 mM, the saturation concentration of UCB in the chloroform phase (26).

that, at a normal plasma albumin concentration of 0.6 mM and a normal maximum plasma UCB concentration of about 20 $\mu$M (55), the concentration of unbound UCB must be about 0.5 nM, of which 83% is $H_2B^o$ at pH 7.4. Therefore, normal plasma is undersaturated with unbound UCB, and would become saturated only if the total bilirubin concentration increased more than 200-fold above normal (to >400 $\mu$M), which rarely occurs (56). Brodersen's own data (Fig. 50 in ref. 52) indicate that, at pH 7.4 and a physiologically low albumin concentration of 0.4 mM, the concentration of unbound UCB does not exceed our solubility limit of 0.1 $\mu$M until total UCB exceeds 500 $\mu$M.

As pH decreases, published reports, with few exceptions (57, 58), demonstrate increased distribution of UCB into membranes of erythrocytes (54, 59, 60), hepatic mitochondria (38, 61), and tissue culture cells (62, 63), as well as phospholipid vesicles (42, 53). Our data (Fig. 7) show a corresponding increase in the proportion of $H_2B^o$ as the pH decreases in the physiological range. These findings are compatible with a mechanism akin to partition into chloroform, involving increasing distribution of the soluble $H_2B^o$ species from aqueous solutions into membranes without formation of precipitates. Wennberg (54) has proposed, by contrast, that the soluble bilirubin monoanion is the form that diffuses into tissues, principally from a highly concentrated pool of $HB^-$ at the aqueous/lipid interface. Our results (Fig. 7), showing that the proportion of $HB^-$ decreases with decreasing pH, are incompatible with this hypothesis.

*Pathogenesis of pigment gallstones* (1–3). Our data indicate that the solubilities of UCB in simple buffered aqueous systems at pH 6 to 8 are less than 1% of the maximum concentrations found in normal human gallbladder bile (35 $\mu$M) or hepatic bile (10 $\mu$M) (64). This indicates that UCB must be solubilized by interaction with other components of bile, principally bile salts (1–3, 5–8, 22, 43, 65, 66), but it is unclear whether those interactions are sufficient to fully solubilize the UCB in bile. The fact that UCB in gallstones is found only as its calcium salts, and not as the diacid (1–3, 67–69), suggests that bile is not supersaturated with UCB per se, and/or that antinucleating factors for UCB are present in bile (69). It indicates also that the solubility products of calcium salts of bilirubin anions, and therefore the unbound concentrations of $Ca^{2+}$, $HB^-$, and $B^=$ must be major determinants of the precipitation of bilirubin in bile (1–3, 69, 70). As our study indicates that the major anion in bile is probably $HB^-$ and that there is little $B^=$ present, one would expect mainly the $Ca(HB^-)_2$ salt to be present in gallstones, as is actually the case (67–69). It remains to extend the present partition method to determine the actual activities of unbound $HB^-$ and $B^=$ in the presence of bile salts and lecithin and the solubility products of the calcium bilirubinates. Our studies demonstrate clearly, however, that the ion products of these salts, and therefore their relative saturation in bile, would increase with increasing bile pH, and that defective acidification of bile in the gallbladder might favor precipitation of calcium bilirubinates, as it does for calcium carbonates (50, 51, 70).

## APPENDIX: DERIVATION OF MODEL AND EQUATIONS

### I. Definitions

Bw = total bilirubin concentration in upper (buffered aqueous) phase; Bc = total bilirubin concentration in the lower (organic $CHCl_3$) phase; P = the aqueous/$CHCl_3$ partition ratio = Bw/Bc. Forms of UCB: $H_2B^o$ = diacid, $HB^-$ = monoanion, $B^=$ = dianion.

1. *Acid–base equilibria*: $(H_2B^o) \rightleftharpoons (HB^-) + (H^+)$ Dissociation constant = $K'_1$. $(HB^-) \rightleftharpoons (B^=) + (H^+)$ Dissociation constant = $K'_2$.

2. *Bilirubin self-associations:* $H_2B^o + H_2B^o \rightleftharpoons (H_2B^o)_2$ Association constant = $k_{00}$. $HB^- + HB^- \rightleftharpoons (HB^-)_2$ Association constant = $k_{11}$. $B^= + B^= \rightleftharpoons (B^=)_2$ Association constant = $k_{22}$. $H_2B^o + HB^- \rightleftharpoons (H_2B^o)(HB^-)$ Association constant = $k_{01}$. $H_2B^o + B^= \rightleftharpoons (H_2B^o)(B^=)$ Association constant = $k_{02}$. $HB^- + B^= \rightleftharpoons (HB^-)(B^=)$ Association constant = $k_{12}$. *It is assumed for these studies that higher aggregates do not occur.*

### II. Assumptions and special considerations

1. Bilirubin diacid ($H_2B^o$) is the only species in the $CHCl_3$ phase, and thus the only one that partitions from the C phase into the aqueous (W) phase. It then ionizes in the W phase according to its intrinsic pK'a values, and the ambient pH in that phase.

2. There is no aggregation of bilirubin in the C phase (43), which therefore contains only $H_2B^o$ monomers.

3. Due to 1 and 2, the activity of $H_2B^o$ in the W phase is regulated by the activity of $H_2B^o$ in the C phase and the intrinsic partition coefficient of $H_2B^o$, Po. Therefore, for any given [Bc], the total concentration of all forms of UCB diacid $[H_2B^o]$ in the W phase is constant at all pH values, and equal to [Bw] at pH $\leq$4.0.

4. The small component of $CHCl_3$ in the aqueous phase, and of water in the $CHCl_3$ phase, has minimal effects on the system with respect to *studies with varied pH and [Bc].*

### III. Mathematical equations describing equilibria

*The general model:*

(1) $[Bw] = [H_2B^o] + [HB^-] + [B^=] + 2[(H_2B^o)_2] + 2[(H_2B^o)(HB^-)] + 2[(H_2B^o)(B^=)] + 2[(HB^-)_2] + 2[(HB^-)(B^=)] + 2[(B^=)_2]$...etc.

Set $[H_2B^o] = a$ (a constant). Then:

(2) $[HB^-] = a \cdot K_1/[H^+]$

(3) $[B^=] = [HB^-] \cdot K_2/[H^+] = a \cdot K_1 \cdot K_2/[H^+]^2$

(4) $[H_2B^o]_2 = a^2 \cdot k_{00}$

(5) $[(H_2B^o)(HB^-)] = k_{01} \cdot a[HB^-] = a^2 \cdot k_{01} \cdot K_1/[H^+]$

(6) $[H_2B^o)(B^=)] = a \cdot k_{02} \cdot [B^=] = a^2 \cdot k_{02} \cdot K_1 \cdot K_2/[H^+]^2$

(7) $[HB^-]_2 = k_{11} \cdot [HB^-]^2 = a^2 \cdot k_{11} \cdot (K_1/[H^+])^2$

(8) $[(HB^-)(B^=) = k_{12} \cdot [HB^-] \cdot [B^=] = a^2 \cdot k_{12} \cdot (K_1)^2 \cdot K_2/[H^+]^3$

(9) $[B^=]_2 = k_{22} \cdot [B^=]^2 = a^2 \cdot k_{22} \cdot (K_1 \cdot K_2)^2/[H^+]^4$

Then (1) becomes:

(10) $[Bw] = a + a \cdot K_1/[H^+] + a \cdot K_1 \cdot K_2/[H^+]^2 + 2a^2 \cdot k_{00} + 2a^2 \cdot k_{01} \cdot K_1/[H^+] + 2a^2 \cdot k_{02} \cdot K_1 \cdot K_2/[H^+]^2 + 2a^2 \cdot k_{11} \cdot (K_1/[H^+])^2 + 2a^2 \cdot k_{12} \cdot (K_1)^2 \cdot K_2/[H^+]^3 + 2a^2 \cdot k_{22} \cdot (K_1 \cdot K_2)^2/[H^+]^4$...etc.

Since the partition ratio, P = Bw/Bc, equation (10) may be rewritten as:

(11) $P = (1/[Bc]) \cdot \{a + a \cdot K_1/[H^+] + a \cdot K_1 \cdot K_2/[H^+]^2 + 2a^2 \cdot k_{00} + 2a^2 \cdot k_{01} \cdot K_1/[H^+] + 2a^2 \cdot k_{02} \cdot K_1 \cdot K_2/[H^+]^2 + 2a^2 \cdot k_{11} \cdot (K_1/[H^+])^2 + 2a^2 \cdot k_{12} \cdot (K_1)^2 \cdot K_2/[H^+]^3 + 2a^2 \cdot k_{22} \cdot (K_1 \cdot K_2)^2/[H^+]^4$...etc.$\}$

Since Po = a/Bc, by substituting $Po \cdot Bc = a$, equation (10) becomes:

(12) $P = Po + Po \cdot K_1/[H^+] + Po \cdot K_1 \cdot K_2/[H^+]^2 + 2(Po)^2 \cdot Bc \cdot k_{00} + 2(Po)^2 \cdot Bc \cdot k_{01} \cdot K_1/[H^+] + 2(Po)^2 \cdot Bc \cdot k_{02} \cdot K_1 \cdot K_2/[H^+]^2 + 2(Po)^2 \cdot Bc \cdot k_{11} \cdot (K_1/[H^+])^2 + 2(Po)^2 \cdot Bc \cdot k_{12} \cdot (K_1)^2 \cdot K_2/[H^+]^3 + 2(Po)^2 \cdot Bc \cdot k_{22} \cdot (K_1 \cdot K_2)^2/[H^+]^4$...etc.

As long as Po is constant, and [Bc] and pH (i.e., $[H^+]$) are known, then all terms in equation (12) are fixed, and we can collect terms in $1/[H^+]$, $1/[H^+]^2$, etc., as well as the terms with no $[H^+]$. Therefore, factoring out Po, we get:

(13) $P = Po \cdot \{Q + R/[H^+] + S/[H^+]^2 + T/[H^+]^3 + U/[H^+]^4$...etc.$\}$
where: $Q = 1 + 2Po \cdot Bc \cdot k_{00}$;
$R = K_1 + 2Po \cdot Bc \cdot k_{01} \cdot K_1$;
$S = K_1 \cdot K_1 + 2Po \cdot Bc \cdot k_{02} \cdot K_1 \cdot K_2 + 2Po \cdot Bc \cdot k_{11} \cdot (K_1)^2$;
$T = 2Po \cdot Bc \cdot k_{12} \cdot (K_1)^2 \cdot K_2$;
$U = 2Po \cdot Bc \cdot k_{22} \cdot (K_1 \cdot K_2)^2$...etc.

Thus, irrespective of what species are considered, and independent of how many aggregates form, the equation for P must have the form of (13), a power series of $1/[H^+]$, for powers of 0 to n. However, the coefficients Q, R, S, T, U...etc. may all be complex quantities, each in part dependent upon [Bc].

Simpler models can be constructed from equation (13) by assuming that certain species are not present in the system, which eliminates the terms that define them in the equation.

B. *Model assuming no self-aggregation of any UCB species.*

If, over the full pH range, the shape of the curve is little affected by varying [Bc], then the $a^2$ terms in (10) must be negligible and there must be little self-aggregation of UCB. In this case, the constants in (13) become $Q^* = 1$, $R^* = K_1$ and $S^* = K_1 \cdot K_2$, and the T and U terms are absent. This yields the simplest model that includes the dianion ($B^=$) and reduces to the equation:

(14) $P = Po + Po \cdot K_1/[H^+] + Po \cdot K_1 \cdot K_2/[H^+]^2$. Converting to logarithms yields the equation:

(15) $\log P = \log Po + \log \{1 + 10^{(pH-A)} + 10^{(2pH-B)}\}$, where: $A = pK_1$ and $B = pK_1 + pK_2$.

For this model, which assumes no aggregates of any forms of UCB, the curve of log P vs. pH should approach a straight line with a slope of 2 at high pH, where the $(10^{(2pH-B)}) \gg (10^{(pH-A)})$. Formation of $(HB^-)(B^=)$ and/or $(B^=)_2$ species would produce a slope greater than 2, which is not allowed by equation (15). Such a higher slope was seen in our study of the dissolution of UCB crystals in the absence of bile salts (5), indicating formation of aggregates in that situation.

C. *Model assuming formation only of the aggregates $(HB^-B^=)$ and $(B^=)_2$.*

If the concentrations of $H_2B^o$ and $HB^-$ in the aqueous phase are very low, and/or the aggregation constants $k_{00}$, $k_{01}$, $k_{02}$, and $k_{11}$ are very low, then there will be negligible concentrations of the aggregates $(H_2B^o)_2$, $(H_2B^o)(HB^-)$, $(H_2B^o)(B^=)$ and $(HB^-)_2$. In this case, changes in [Bc] will have little effect on the shape of the curve over the range of pH values below $pK_1 + 1$. As in the model under B, above, the constants of equation (13) become $Q^* = 1$, $R^* = K_1$ and $S^* = K_2 \cdot K_2$. Terms for $(HB^-)(B^=)$ and $(B^=)_2$, contained in T and U, must, however, now be included. To do this, we rewrite equation (13) in terms of measured variables:

(16) $P = Po \cdot \{1 + K_1/[H^+] + K_1 \cdot K_2/[H^+]^2 + Bc \cdot T^*/[H^+]^3 + Bc \cdot U^*/[H^+]^4\}$ where: $T^* = 2Po \cdot k_{12} \cdot (K_1)^2 \cdot K_2$ and $U^* = 2Po \cdot k_{22} \cdot (K_1 \cdot K_2)^2$.

Converting (16) to a logarithmic function yields the equation:

(17) $\log P = \log Po + \log \{1 + 10^{(pH-A)} + 10^{(2pH-B)} + Bc \cdot 10^{(3pH-C)} + Bc \cdot 10^{(4pH-D)}\}$ where: $A = pK_1$; $B = pK_1 + pK_2$;
$C = pk_{12} + 2pK_1 + pK_2 - \log(2Po)$; and
$D = pk_{22} + 2(pK_1 + pK_2) - \log(2Po)$.

In this equation, the only variables are pH and Bc.

D. *Estimation of solubilities in aqueous phases.*

Consistent with our assumptions, the saturation solubility of UCB in water ($[Bw]_{satd}$), at any pH, can be calculated from the value of P at that pH and the saturation solubility of UCB in $CHCl_3$, $[Bc]_{satd}$. If $[Bc]_{satd}$ can be measured, then $[Bw]_{satd} = P \cdot [Bc]_{satd}$. Due to the presence of the $CHCl_3$ phase during determination of P, the aqueous partition phase is actually saturated with a small proportion of $CHCl_3$. Since the concentration of $CHCl_3$ in water is minute, $[Bw]_{satd}$ in the aqueous phase in the absence of $CHCl_3$ is likely to be close to that determined as above in the presence of $CHCl_3$.

We are grateful to Dr. Chun Chiu Chan, Dept. of Pharmaceutics, School of Pharmacy, University of Wisconsin, Madison, WI, for his performance of the computer-analyses of our data. We are appreciative also of the helpful comments by Dr. Robert V. Rege, Department of Surgery, Northwestern University, Chicago, IL. Support for this project was provided by extramural research grant 2RO1-DK32130 from the National Institutes of Health, Bethesda, MD, and by a Medical Investigator Award from the U.S. Department of Veterans Affairs.

*Manuscript received March 1991, in revised form 9 January 1992, and in re-revised form 23 March 1992.*

## REFERENCES

1. Ostrow, J. D. 1984. The etiology of pigment gallstones. *Hepatology.* **4:** 215S–222S.
2. Cahalane, M. J., M. W. Neubrand, and M. C. Carey. 1988. Physical-chemical pathogenesis of pigment gallstones. *Semin. Liver Dis.* **8:** 317–328.
3. Crowther, R. S., and R. D. Soloway. 1990. Pigment gallstone pathogenesis: from man to molecules. *Semin. Liver Dis.* **10:** 171–180.
4. Brodersen, R., and L. Stern. 1990. Review article. Deposition of bilirubin acid in the central nervous system—a hypothesis for the development of kernicterus. *Acta Paediatr. Scand.* **79:** 12–19.
5. Ostrow, J. D., L. Celic, and P. Mukerjee. 1988. Molecular and micellar associations in the pH-dependent stable and metastable dissolution of unconjugated bilirubin by bile salts. *J. Lipid Res.* **29:** 335–348.
6. Nakama, T. 1976. Significance of biliary cholesterol and bilirubin in gallstone formation. *Fukuoka Acta Med.* **67:** 413–441.
7. Nakama, T., T. Furusawa, H. Itoh, and T. Hisadome.

1979. Correlation of cholesterol and bilirubin solubilization in bile salt solution. *Gastroenterol. Jpn.* **6:** 565–572.
8. Wosiewitz, U., and S. Schroebler. 1979. Solubilization of unconjugated bilirubin by bile salts. *Experientia.* **35:** 717–718.
9. Overbeek, J. T. G., C. L. J. Vink, and H. Deenstra. 1955. The solubility of bilirubin. *Rec. Trav. Chim. Pays-Bas.* **74:** 81–84.
10. Ostrow, J. D., T. J. Devers, and D. Gallo. 1977. Determinants of the solubility of unconjugated bilirubin in bile: relationship to pigment gallstones. *In* Chemistry and Physiology of Bile Pigments. P. D. Berk and N. I. Berlin, editors. National Institutes of Health, DHEW, Fogarty International Conference Proceedings, Bethesda, MD. 404–409.
11. Brodersen, R. 1979. Bilirubin solubility and interaction with albumin and phospholipid. *J. Biol. Chem.* **254:** 2364–2369.
12. Brodersen, R. 1986. Aqueous solubility, albumin binding, and tissue distribution of bilirubin. *In* Bile Pigments and Jaundice; Molecular, Metabolic and Medical Aspects. J. D. Ostrow, editor. Marcel Dekker, New York, NY. 157–181.
13. Berman, M. D., A. P. Koretsky, and M. C. Carey. 1980. Influence of pH on the solubility of unconjugated bilirubin (UCB) in artificial bile solutions. *Gastroenterology.* **78:** 1141 (abstr.).
14. Moroi, Y., R. Matuura, and T. Hisadome. 1985. Bilirubin in aqueous solution. Absorption spectrum, aqueous solubility, and dissociation constants. *Bull. Chem. Soc. Japan.* **58:** 1426–1431.
15. Tera, H. 1960. Stratification of human gallbladder bile in vivo. *Acta Chir. Scand.* **256: (Suppl.)** 1–85.
16. Mysels, K. J., and J. W. McBain. 1948. Variability and inhomogeneity of aluminum dilaurate. *J. Phys. Coll. Chem.* **52:** 1471–1481.
17. Nancollas, G. H. 1984. Crystallization in bile. *Hepatology.* **4:** 169S–172S.
18. Lucassen, J. 1966. Hydrolysis and precipitates in carboxylate soap solutions. *J. Phys. Chem.* **70:** 1824–1830.
19. Rosoff, M., J. H. Schulman, H. Erbring, and W. Winkler. 1967. Surface activity of metastable colloidal solutions. Part I. Experimental results with solutions of aescin. *Kolloid Z. Z. Polym.* **216–217:** 347–355.
20. Blanckaert, N., and K. P. M. Heirwegh. 1986. Analysis and preparation of bilirubins and biliverdins. *In* Bile Pigments and Jaundice; Molecular, Metabolic and Medical Aspects. J. D. Ostrow, editor, Marcel Dekker, New York. 31–80.
21. Brodersen, R. 1966. Dimerisation of bilirubin anion in aqueous solution. *Acta Chem. Scand.* **20:** 2895–2896.
22. Carey, M. C., and A. P. Koretsky. 1979. Self-association of unconjugated bilirubin IXα in aqueous solution at pH 10.0, and physical-chemical interactions with bile salt monomers and micelles. *Biochem. J.* **179:** 675–689.
23. McDonagh, A. F., and F. Assisi. 1972. The ready isomerization of bilirubin IXα in aqueous solution. *Biochem. J.* **129:** 797–800.
24. Michaelsson, M. 1961. Bilirubin determination in serum and urine. Studies on diazo methods and a new copper-azopigment method. *Scand. J. Clin. Lab. Invest.* **13: (Suppl. 56):** 1–80.
25. Snedecor, G. W., and W. G. Cochran. 1967. Statistical Methods. 6th edition. Iowa State University Press, Ames, IA. 59–60, 94–96, and 114–118.
26. Hahm, J. S., J. D. Ostrow, P., Mukerjee, and L. Celic. 1986. Solubility and pK'a of unconjugated bilirubin in aqueous buffer and bile salt solutions, determined by isoextraction from chloroform. *Hepatology.* **6:** 1185 (abstr.).
27. Christian, S. D., H. E. Affspring, and S. A. Taylor. 1963. Dissolved water in partition equilibriums of carboxylic acids. *J. Phys. Chem.* **67:** 187–189.
28. Goodman, D. S. 1958. The distribution of fatty acids between n-heptane and aqueous phosphate buffer. *J. Am. Chem. Soc.* **80:** 3887–3892.
29. Goodman, D. S. 1958. The interaction of human serum albumin with long chain fatty acid anions. *J. Am. Chem. Soc.* **80:** 3893–3898.
30. Mukerjee, P. 1965. Dimerization of anions of long-chain fatty acids in aqueous solutions and the hydrophobic properties of the acids. *J. Phys. Chem.* **69:** 2821–2828.
31. Simpson, R. B., J. D. Ashbrook, E. C. Santos, and A. A. Spector. 1974. Partition of fatty acids. *J. Lipid Res.* **15:** 415–422.
32. Smith, R., and C. Tanford. 1973. Hydrophobicity of long-chain n-alkyl carboxylic acids, as measured by their distribution between heptane and aqueous solutions. *Proc. Natl. Acad. Sci. USA.* **70:** 289–293.
33. Mukerjee, P., and A. K. Ghosh. 1970. The "isoextraction" method and the study of self-association of methylene blue in aqueous solutions. *J. Am. Chem. Soc.* **92:** 6403–6407.
34. Ghosh, A. K., and P. Mukerjee. 1970. Multiple association equilibria in the self-association of methylene blue and other dyes. *J. Am. Chem. Soc.* **92:** 6407–6412.
35. Ghosh, A. K., and P. Mukerjee. 1970. Ionic strength effects on the activity coefficient of methylene blue and its self-association. *J. Am. Chem. Soc.* **92:** 6413–6415.
36. Ghosh, A. K. 1970. Study of the self-association of methylene blue from protonation equilibria. *J. Am. Chem. Soc.* **92:** 6415–6418.
37. Mukerjee, P., and A. K. Ghosh. 1970. Thermodynamic aspects of the self-association and hydrophobic bonding of methylene blue. A model system for stacking interactions. *J. Am. Chem. Soc.* **92:** 6418–6424.
38. Brodersen, R., and I. Vind. 1963. Chloroform extraction of serum bilirubin in relationship to its binding to proteins. *Scand. J. Clin. Lab. Invest.* **15:** 107–114.
39. Stephen, H., and T. Stephen, editors. 1963. Solubilities of Inorganic and Organic Compounds. Vol. I, Part 1. MacMillian, New York, NY.
40. Hildebrand, J. H., J. M. Prausnitz, and R. L. Scott. 1970. Regular and Regulated Solutions; the Solubility of Gases, Liquids and Solids. Van Nostrand-Reinhold, New York, NY, 130–135.
41. Mukerjee, P., and Y. Moroi. 1978. Cell for isoextraction studies and determination of some acid dissociation constants. *Anal. Chem.* **50:** 1589–1591.
42. Tipping, E., B. Ketterer, and L. Christodoulides. 1979. Interactions of small molecules with phospholipid bilayers. Binding to egg phosphatidylcholine of some organic anions. (bromsulphophthalein, oestrone sulphate, haem and bilirubin) that bind to ligandin and aminoazo dye-binding protein A. *Biochem. J.* **180:** 327–337.
43. Carey, M. C., and W. Spivak. 1986. Physical chemistry of bile pigments and porphyrins with particular reference to bile. *In* Bile Pigments and Jaundice; Molecular, Metabolic and Medical Aspects. J. D. Ostrow, editor. Marcel Dekker, New York, NY. 81–132.
44. Falk, H. 1986. Molecular structure of bile pigments. *In* Bile Pigments and Jaundice; Molecular, Metabolic and Medical Aspects. J. D. Ostrow, editor. Marcel Dekker, New York, NY. 7–29.
45. Tiribelli, C., and J. D. Ostrow. 1990. New concepts in bilirubin chemistry, transport and metabolism: report of the International Bilirubin Workshop, April 6–8, 1989,

Trieste, Italy. *Hepatology.* **11:** 303–313.
46. Hansen, P. E., H. Thiessen, and R. Brodersen. 1979. Bilirubin acidity; titrimetric and $^{13}$C-NMR studies. *Acta Chem. Scand.* **B33:** 281–293.
47. Robinson, R. A., and R. H. Stokes. 1959. Electrolyte Solutions. 2nd Edition. Butterworths, London. 346–350 and 527–528.
48. Adamson, A. W. 1967. Physical Chemistry of Surfaces. 3rd Edition. Interscience, New York. 334.
49. Mukerjee, P. 1972. Thermodynamic aspects of solubility of small particles. *J. Pharm. Sci.* **61:** 478–479.
50. Shiffman, M. L., and E. W. Moore. 1988. $H^+$ ion secretion by the human gallbladder in patients with and without gallstones. *Hepatology.* **8:** 1223 (Abstr.).
51. Knyrim, K., and N. Vakil. 1990. The effects of synthetic human secretin on calcium carbonate solubility in human bile. *Gastroenterology.* **9:** 1445–1451.
52. Brodersen, R. 1979. Binding of bilirubin to albumin; implications for prevention of bilirubin encephalopathy in the newborn. *CRC Crit. Rev. Clin. Lab. Sci.* **11:** 305–399.
53. Eriksen, E. F., H. Danielsen, and R. Brodersen. 1981. Bilirubin-liposome interaction. Binding of bilirubin dianion, protonization, and aggregation of bilirubin diacid. *J. Biol. Chem.* **256:** 4269–4274.
54. Wennberg, R. P. 1988. The importance of free bilirubin acid salt in bilirubin uptake by erythrocytes and mitochondria. *Pediatr. Res.* **23:** 443–447.
55. Okolicsanyi, L., G. Nassuato, M. Muraca, R. Orlando, R. M. Iemmolo, F. Lirussi, and M. Strazzabosco. 1988. Epidemiology of unconjugated hyperbilirubinemia: revisited. *Semin. Liver Dis.* **8:** 179–182.
56. Kim, M. H., J. J. Yoon, J. Sher, and A. K. Brown. 1980. Lack of predictive indices in kernicterus. A comparison of clinical and pathological factors in infants with and without kernicterus. *Pediatrics.* **66:** 552–558.
57. Bratlid, D. 1972. Bilirubin binding by human erythrocytes. *Scand. J. Clin. Lab. Invest.* **29:** 91–97.
58. Kapoor, C. L., C. R. Krishna Murti, and P. C. Bajpai. 1973. Uptake and release of bilirubin by skin. *Biochem. J.* **136:** 35–43.
59. Sato, H., and S. Kashiwamata. 1983. Interaction of bilirubin with human erythrocyte membranes. *Biochem. J.* **210:** 489–496.
60. Wennberg, R., and L. F. Rasmussen. 1978. Factors determining the cellular uptake of bilirubin. *Pediatr. Res.* **12:** 536 (Abstract).
61. Odell, G. B. 1965. Influence of pH on distribution of bilirubin between albumin and mitochondria. *Proc. Soc. Exp. Biol. Med.* **120:** 352–354.
62. Nelson, T., J. Jacobsen, and R. P. Wennberg. 1974. Effect of pH on the interaction of bilirubin with albumin and tissue culture cells. *Pediatr. Res.* **8:** 963–967.
63. Silberberg, D. H., L. Johnson, and L. Ritter. 1970. Factors influencing toxicity of bilirubin in cerebellum tissue culture. *J. Pediatr.* **77:** 386–396.
64. Fevery, J., N. Blanckaert, P. LeRoy, R. Michiels, and K. P. M. Heirwegh. 1983. Analysis of bilirubins in biological fluids by extraction and thin-layer chromatography of the intact tetrapyrroles: application to bile of patients with Gilbert's syndrome, hemolysis or cholelithiasis. *Hepatology.* **3:** 177–183.
65. Rege, R. V., C. C. Webster, and J. D. Ostrow. 1987. Enzymatic oxidation of unconjugated bilirubin to assess its interactions with taurocholate. *J. Lipid Res.* **28:** 673–683.
66. Rege, R. V., C. C. Webster, and J. D. Ostrow. 1988. Interactions of unconjugated bilirubin with bile salts. *J. Lipid Res.* **29:** 1289–1296.
67. Bogren, H., and K. Larsson. 1963. On the pigment in biliary calculi. *Scand. J. Clin. Lab. Invest.* **15:** 569–572.
68. Sutor, D. J., and L. I. Wilkie. 1977. The crystalline salts of calcium bilirubinate in gallstones. *Clin. Sci. Mol. Med.* **53:** 101–103.
69. Ostrow, J. D. 1990. Unconjugated bilirubin and cholesterol gallstone formation. *Hepatology.* **12:** 219S–226S.
70. Moore, E. W. 1990. Biliary calcium and gallstone formation. *Hepatology.* **12:** 206S–218S.